BABAR-PUB-12/011 SLAC-PUB-15192

Observation of Time Reversal Violation in the B^0 Meson System

J. P. Lees,[1] V. Poireau,[1] V. Tisserand,[1] J. Garra Tico,[2] E. Grauges,[2] A. Palano[ab],[3] G. Eigen,[4] B. Stugu,[4] D. N. Brown,[5] L. T. Kerth,[5] Yu. G. Kolomensky,[5] G. Lynch,[5] H. Koch,[6] T. Schroeder,[6] D. J. Asgeirsson,[7] C. Hearty,[7] T. S. Mattison,[7] J. A. McKenna,[7] R. Y. So,[7] A. Khan,[8] V. E. Blinov,[9] A. R. Buzykaev,[9] V. P. Druzhinin,[9] V. B. Golubev,[9] E. A. Kravchenko,[9] A. P. Onuchin,[9] S. I. Serednyakov,[9] Yu. I. Skovpen,[9] E. P. Solodov,[9] K. Yu. Todyshev,[9] A. N. Yushkov,[9] M. Bondioli,[10] D. Kirkby,[10] A. J. Lankford,[10] M. Mandelkern,[10] H. Atmacan,[11] J. W. Gary,[11] F. Liu,[11] O. Long,[11] G. M. Vitug,[11] C. Campagnari,[12] T. M. Hong,[12] D. Kovalskyi,[12] J. D. Richman,[12] C. A. West,[12] A. M. Eisner,[13] J. Kroseberg,[13] W. S. Lockman,[13] A. J. Martinez,[13] B. A. Schumm,[13] A. Seiden,[13] D. S. Chao,[14] C. H. Cheng,[14] B. Echenard,[14] K. T. Flood,[14] D. G. Hitlin,[14] P. Ongmongkolkul,[14] F. C. Porter,[14] A. Y. Rakitin,[14] R. Andreassen,[15] Z. Huard,[15] B. T. Meadows,[15] M. D. Sokoloff,[15] L. Sun,[15] P. C. Bloom,[16] W. T. Ford,[16] A. Gaz,[16] U. Nauenberg,[16] J. G. Smith,[16] S. R. Wagner,[16] R. Ayad,[17,*] W. H. Toki,[17] B. Spaan,[18] K. R. Schubert,[19] R. Schwierz,[19] D. Bernard,[20] M. Verderi,[20] P. J. Clark,[21] S. Playfer,[21] D. Bettoni[a],[22] C. Bozzi[a],[22] R. Calabrese[ab],[22] G. Cibinetto[ab],[22] E. Fioravanti[ab],[22] I. Garzia[ab],[22] E. Luppi[ab],[22] M. Munerato[ab],[22] L. Piemontese[a],[22] V. Santoro[a],[22] R. Baldini-Ferroli,[23] A. Calcaterra,[23] R. de Sangro,[23] G. Finocchiaro,[23] P. Patteri,[23] I. M. Peruzzi,[23,†] M. Piccolo,[23] M. Rama,[23] A. Zallo,[23] R. Contri[ab],[24] E. Guido[ab],[24] M. Lo Vetere[ab],[24] M. R. Monge[ab],[24] S. Passaggio[a],[24] C. Patrignani[ab],[24] E. Robutti[a],[24] B. Bhuyan,[25] V. Prasad,[25] C. L. Lee,[26] M. Morii,[26] A. J. Edwards,[27] A. Adametz,[28] U. Uwer,[28] H. M. Lacker,[29] T. Lueck,[29] P. D. Dauncey,[30] U. Mallik,[31] C. Chen,[32] J. Cochran,[32] W. T. Meyer,[32] S. Prell,[32] A. E. Rubin,[32] A. V. Gritsan,[33] Z. J. Guo,[33] N. Arnaud,[34] M. Davier,[34] D. Derkach,[34] G. Grosdidier,[34] F. Le Diberder,[34] A. M. Lutz,[34] B. Malaescu,[34] P. Roudeau,[34] M. H. Schune,[34] A. Stocchi,[34] G. Wormser,[34] D. J. Lange,[35] D. M. Wright,[35] C. A. Chavez,[36] J. P. Coleman,[36] J. R. Fry,[36] E. Gabathuler,[36] D. E. Hutchcroft,[36] D. J. Payne,[36] C. Touramanis,[36] A. J. Bevan,[37] F. Di Lodovico,[37] R. Sacco,[37] M. Sigamani,[37] G. Cowan,[38] D. N. Brown,[39] C. L. Davis,[39] A. G. Denig,[40] M. Fritsch,[40] W. Gradl,[40] K. Griessinger,[40] A. Hafner,[40] E. Prencipe,[40] R. J. Barlow,[41,‡] G. Jackson,[41] G. D. Lafferty,[41] E. Behn,[42] R. Cenci,[42] B. Hamilton,[42] A. Jawahery,[42] D. A. Roberts,[42] C. Dallapiccola,[43] R. Cowan,[44] D. Dujmic,[44] G. Sciolla,[44] R. Cheaib,[45] D. Lindemann,[45] P. M. Patel,[45,§] S. H. Robertson,[45] P. Biassoni[ab],[46] N. Neri[a],[46] F. Palombo[ab],[46] S. Stracka[ab],[46] L. Cremaldi,[47] R. Godang,[47,¶] R. Kroeger,[47] P. Sonnek,[47] D. J. Summers,[47] X. Nguyen,[48] M. Simard,[48] P. Taras,[48] G. De Nardo[ab],[49] D. Monorchio[ab],[49] G. Onorato[ab],[49] C. Sciacca[ab],[49] M. Martinelli,[50] G. Raven,[50] C. P. Jessop,[51] J. M. LoSecco,[51] W. F. Wang,[51] K. Honscheid,[52] R. Kass,[52] J. Brau,[53] R. Frey,[53] N. B. Sinev,[53] D. Strom,[53] E. Torrence,[53] E. Feltresi[ab],[54] N. Gagliardi[ab],[54] M. Margoni[ab],[54] M. Morandin[a],[54] A. Pompili[a],[54] M. Posocco[a],[54] M. Rotondo[a],[54] G. Simi[a],[54] F. Simonetto[ab],[54] R. Stroili[ab],[54] S. Akar,[55] E. Ben-Haim,[55] M. Bomben,[55] G. R. Bonneaud,[55] H. Briand,[55] G. Calderini,[55] J. Chauveau,[55] O. Hamon,[55] Ph. Leruste,[55] G. Marchiori,[55] J. Ocariz,[55] S. Sitt,[55] M. Biasini[ab],[56] E. Manoni[ab],[56] S. Pacetti[ab],[56] A. Rossi[ab],[56] C. Angelini[ab],[57] G. Batignani[ab],[57] S. Bettarini[ab],[57] M. Carpinelli[ab],[57,**] G. Casarosa[ab],[57] A. Cervelli[ab],[57] F. Forti[ab],[57] M. A. Giorgi[ab],[57] A. Lusiani[ac],[57] B. Oberhof[ab],[57] E. Paoloni[ab],[57] A. Perez[a],[57] G. Rizzo[ab],[57] J. J. Walsh[a],[57] D. Lopes Pegna,[58] J. Olsen,[58] A. J. S. Smith,[58] A. V. Telnov,[58] F. Anulli[a],[59] R. Faccini[ab],[59] F. Ferrarotto[a],[59] F. Ferroni[ab],[59] M. Gaspero[ab],[59] L. Li Gioi[a],[59] M. A. Mazzoni[a],[59] G. Piredda[a],[59] C. Bünger,[60] O. Grünberg,[60] T. Hartmann,[60] T. Leddig,[60] H. Schröder,[60,§] C. Voss,[60] R. Waldi,[60] T. Adye,[61] E. O. Olaiya,[61] F. F. Wilson,[61] S. Emery,[62] G. Hamel de Monchenault,[62] G. Vasseur,[62] Ch. Yèche,[62] D. Aston,[63] D. J. Bard,[63] R. Bartoldus,[63] J. F. Benitez,[63] C. Cartaro,[63] M. R. Convery,[63] J. Dorfan,[63] G. P. Dubois-Felsmann,[63] W. Dunwoodie,[63] M. Ebert,[63] R. C. Field,[63] M. Franco Sevilla,[63] B. G. Fulsom,[63] A. M. Gabareen,[63] M. T. Graham,[63] P. Grenier,[63] C. Hast,[63] W. R. Innes,[63] M. H. Kelsey,[63] P. Kim,[63] M. L. Kocian,[63] D. W. G. S. Leith,[63] P. Lewis,[63] B. Lindquist,[63] S. Luitz,[63] V. Luth,[63] H. L. Lynch,[63] D. B. MacFarlane,[63] D. R. Muller,[63] H. Neal,[63] S. Nelson,[63] M. Perl,[63] T. Pulliam,[63] B. N. Ratcliff,[63] A. Roodman,[63] A. A. Salnikov,[63] R. H. Schindler,[63] A. Snyder,[63] D. Su,[63] M. K. Sullivan,[63] J. Va'vra,[63] A. P. Wagner,[63] W. J. Wisniewski,[63] M. Wittgen,[63] D. H. Wright,[63] H. W. Wulsin,[63] C. C. Young,[63] V. Ziegler,[63] W. Park,[64] M. V. Purohit,[64] R. M. White,[64] J. R. Wilson,[64] A. Randle-Conde,[65] S. J. Sekula,[65] M. Bellis,[66] P. R. Burchat,[66] T. S. Miyashita,[66] E. M. T. Puccio,[66] M. S. Alam,[67] J. A. Ernst,[67] R. Gorodeisky,[68] N. Guttman,[68] D. R. Peimer,[68] A. Soffer,[68] P. Lund,[69] S. M. Spanier,[69] J. L. Ritchie,[70]

arXiv:1207.5832v3 [hep-ex] 6 Oct 2012

A. M. Ruland,[70] R. F. Schwitters,[70] B. C. Wray,[70] J. M. Izen,[71] X. C. Lou,[71] F. Bianchi[ab],[72] D. Gamba[ab],[72] S. Zambito[ab],[72] L. Lanceri[ab],[73] L. Vitale[ab],[73] J. Bernabeu,[74] F. Martinez-Vidal,[74] A. Oyanguren,[74] P. Villanueva-Perez,[74] H. Ahmed,[75] J. Albert,[75] Sw. Banerjee,[75] F. U. Bernlochner,[75] H. H. F. Choi,[75] G. J. King,[75] R. Kowalewski,[75] M. J. Lewczuk,[75] I. M. Nugent,[75] J. M. Roney,[75] R. J. Sobie,[75] N. Tasneem,[75] T. J. Gershon,[76] P. F. Harrison,[76] T. E. Latham,[76] H. R. Band,[77] S. Dasu,[77] Y. Pan,[77] R. Prepost,[77] and S. L. Wu[77]

(The *BABAR* Collaboration)

[1]*Laboratoire d'Annecy-le-Vieux de Physique des Particules (LAPP), Université de Savoie, CNRS/IN2P3, F-74941 Annecy-Le-Vieux, France*
[2]*Universitat de Barcelona, Facultat de Fisica, Departament ECM, E-08028 Barcelona, Spain*
[3]*INFN Sezione di Bari[a]; Dipartimento di Fisica, Università di Bari[b], I-70126 Bari, Italy*
[4]*University of Bergen, Institute of Physics, N-5007 Bergen, Norway*
[5]*Lawrence Berkeley National Laboratory and University of California, Berkeley, California 94720, USA*
[6]*Ruhr Universität Bochum, Institut für Experimentalphysik 1, D-44780 Bochum, Germany*
[7]*University of British Columbia, Vancouver, British Columbia, Canada V6T 1Z1*
[8]*Brunel University, Uxbridge, Middlesex UB8 3PH, United Kingdom*
[9]*Budker Institute of Nuclear Physics, Novosibirsk 630090, Russia*
[10]*University of California at Irvine, Irvine, California 92697, USA*
[11]*University of California at Riverside, Riverside, California 92521, USA*
[12]*University of California at Santa Barbara, Santa Barbara, California 93106, USA*
[13]*University of California at Santa Cruz, Institute for Particle Physics, Santa Cruz, California 95064, USA*
[14]*California Institute of Technology, Pasadena, California 91125, USA*
[15]*University of Cincinnati, Cincinnati, Ohio 45221, USA*
[16]*University of Colorado, Boulder, Colorado 80309, USA*
[17]*Colorado State University, Fort Collins, Colorado 80523, USA*
[18]*Technische Universität Dortmund, Fakultät Physik, D-44221 Dortmund, Germany*
[19]*Technische Universität Dresden, Institut für Kern- und Teilchenphysik, D-01062 Dresden, Germany*
[20]*Laboratoire Leprince-Ringuet, Ecole Polytechnique, CNRS/IN2P3, F-91128 Palaiseau, France*
[21]*University of Edinburgh, Edinburgh EH9 3JZ, United Kingdom*
[22]*INFN Sezione di Ferrara[a]; Dipartimento di Fisica, Università di Ferrara[b], I-44100 Ferrara, Italy*
[23]*INFN Laboratori Nazionali di Frascati, I-00044 Frascati, Italy*
[24]*INFN Sezione di Genova[a]; Dipartimento di Fisica, Università di Genova[b], I-16146 Genova, Italy*
[25]*Indian Institute of Technology Guwahati, Guwahati, Assam, 781 039, India*
[26]*Harvard University, Cambridge, Massachusetts 02138, USA*
[27]*Harvey Mudd College, Claremont, California 91711, USA*
[28]*Universität Heidelberg, Physikalisches Institut, Philosophenweg 12, D-69120 Heidelberg, Germany*
[29]*Humboldt-Universität zu Berlin, Institut für Physik, Newtonstr. 15, D-12489 Berlin, Germany*
[30]*Imperial College London, London, SW7 2AZ, United Kingdom*
[31]*University of Iowa, Iowa City, Iowa 52242, USA*
[32]*Iowa State University, Ames, Iowa 50011-3160, USA*
[33]*Johns Hopkins University, Baltimore, Maryland 21218, USA*
[34]*Laboratoire de l'Accélérateur Linéaire, IN2P3/CNRS et Université Paris-Sud 11, Centre Scientifique d'Orsay, B. P. 34, F-91898 Orsay Cedex, France*
[35]*Lawrence Livermore National Laboratory, Livermore, California 94550, USA*
[36]*University of Liverpool, Liverpool L69 7ZE, United Kingdom*
[37]*Queen Mary, University of London, London, E1 4NS, United Kingdom*
[38]*University of London, Royal Holloway and Bedford New College, Egham, Surrey TW20 0EX, United Kingdom*
[39]*University of Louisville, Louisville, Kentucky 40292, USA*
[40]*Johannes Gutenberg-Universität Mainz, Institut für Kernphysik, D-55099 Mainz, Germany*
[41]*University of Manchester, Manchester M13 9PL, United Kingdom*
[42]*University of Maryland, College Park, Maryland 20742, USA*
[43]*University of Massachusetts, Amherst, Massachusetts 01003, USA*
[44]*Massachusetts Institute of Technology, Laboratory for Nuclear Science, Cambridge, Massachusetts 02139, USA*
[45]*McGill University, Montréal, Québec, Canada H3A 2T8*
[46]*INFN Sezione di Milano[a]; Dipartimento di Fisica, Università di Milano[b], I-20133 Milano, Italy*
[47]*University of Mississippi, University, Mississippi 38677, USA*
[48]*Université de Montréal, Physique des Particules, Montréal, Québec, Canada H3C 3J7*
[49]*INFN Sezione di Napoli[a]; Dipartimento di Scienze Fisiche, Università di Napoli Federico II[b], I-80126 Napoli, Italy*
[50]*NIKHEF, National Institute for Nuclear Physics and High Energy Physics, NL-1009 DB Amsterdam, The Netherlands*
[51]*University of Notre Dame, Notre Dame, Indiana 46556, USA*
[52]*Ohio State University, Columbus, Ohio 43210, USA*
[53]*University of Oregon, Eugene, Oregon 97403, USA*

[54]INFN Sezione di Padova[a]; Dipartimento di Fisica, Università di Padova[b], I-35131 Padova, Italy
[55]Laboratoire de Physique Nucléaire et de Hautes Energies,
IN2P3/CNRS, Université Pierre et Marie Curie-Paris6,
Université Denis Diderot-Paris7, F-75252 Paris, France
[56]INFN Sezione di Perugia[a]; Dipartimento di Fisica, Università di Perugia[b], I-06100 Perugia, Italy
[57]INFN Sezione di Pisa[a]; Dipartimento di Fisica,
Università di Pisa[b]; Scuola Normale Superiore di Pisa[c], I-56127 Pisa, Italy
[58]Princeton University, Princeton, New Jersey 08544, USA
[59]INFN Sezione di Roma[a]; Dipartimento di Fisica,
Università di Roma La Sapienza[b], I-00185 Roma, Italy
[60]Universität Rostock, D-18051 Rostock, Germany
[61]Rutherford Appleton Laboratory, Chilton, Didcot, Oxon, OX11 0QX, United Kingdom
[62]CEA, Irfu, SPP, Centre de Saclay, F-91191 Gif-sur-Yvette, France
[63]SLAC National Accelerator Laboratory, Stanford, California 94309 USA
[64]University of South Carolina, Columbia, South Carolina 29208, USA
[65]Southern Methodist University, Dallas, Texas 75275, USA
[66]Stanford University, Stanford, California 94305-4060, USA
[67]State University of New York, Albany, New York 12222, USA
[68]Tel Aviv University, School of Physics and Astronomy, Tel Aviv, 69978, Israel
[69]University of Tennessee, Knoxville, Tennessee 37996, USA
[70]University of Texas at Austin, Austin, Texas 78712, USA
[71]University of Texas at Dallas, Richardson, Texas 75083, USA
[72]INFN Sezione di Torino[a]; Dipartimento di Fisica Sperimentale, Università di Torino[b], I-10125 Torino, Italy
[73]INFN Sezione di Trieste[a]; Dipartimento di Fisica, Università di Trieste[b], I-34127 Trieste, Italy
[74]IFIC, Universitat de Valencia-CSIC, E-46071 Valencia, Spain
[75]University of Victoria, Victoria, British Columbia, Canada V8W 3P6
[76]Department of Physics, University of Warwick, Coventry CV4 7AL, United Kingdom
[77]University of Wisconsin, Madison, Wisconsin 53706, USA

(Dated: July 20, 2012)

Although CP violation in the B meson system has been well established by the B factories, there has been no direct observation of time reversal violation. The decays of entangled neutral B mesons into definite flavor states (B^0 or $\overline{B}^0$), and $J/\psi K^0_L$ or $c\overline{c}K^0_S$ final states (referred to as B_+ or B_-), allow comparisons between the probabilities of four pairs of T-conjugated transitions, for example, $\overline{B}^0 \to B_-$ and $B_- \to \overline{B}^0$, as a function of the time difference between the two B decays. Using 468 million $B\overline{B}$ pairs produced in $\Upsilon(4S)$ decays collected by the *BABAR* detector at SLAC, we measure T-violating parameters in the time evolution of neutral B mesons, yielding $\Delta S^+_T = -1.37 \pm 0.14$ (stat.)$\pm$ 0.06 (syst.) and $\Delta S^-_T = 1.17 \pm 0.18$ (stat.) $\pm$ 0.11 (syst.). These nonzero results represent the first direct observation of T violation through the exchange of initial and final states in transitions that can only be connected by a T-symmetry transformation.

PACS numbers: 13.25.Ft, 11.30.Er, 12.15.Ff, 14.40.Lb

The observations of CP-symmetry breaking, first in neutral K decays [1] and more recently in B mesons [2, 3], are consistent with the standard model (SM) mechanism of the three-family Cabibbo-Kobayashi-Maskawa (CKM) quark-mixing matrix being the dominant source of CP violation [4]. Local Lorentz invariant quantum field theories imply CPT invariance [5], in accordance with all experimental evidence [6, 7]. Hence, it is expected that the CP-violating weak interaction also violates time reversal invariance.

To date, the only evidence related to T violation has been found in the neutral K system, where a difference between the probabilities of $K^0 \to \overline{K}^0$ and $\overline{K}^0 \to K^0$ transitions for a given elapsed time has been measured [8]. This flavor mixing asymmetry is both CP- and T-violating (the two transformations lead to the same observation), independent of time, and requires a nonzero decay width difference $\Delta\Gamma_K$ between the neutral K mass eigenstates to be observed [9–11]. The dependence with $\Delta\Gamma_K$ has aroused controversy in the interpretation of this observable [7, 10–12]. In the neutral B and B_s systems, where $\Delta\Gamma_d$ and $\Delta\Gamma_s$ are negligible and significantly smaller, respectively, the flavor mixing asymmetry is much more difficult to detect [13]. Experiments that could provide direct evidence supporting T non-invariance, without using an observation which also violates CP, involve either nonvanishing expectation values of T-odd observables, or the exchange of initial and final states, which are not CP conjugates to each other, in the time evolution for transition processes. Among the former, there exist upper limits for electric dipole moments of the neutron and the electron [14]. The latter, requiring neutrinos or unstable particles, are particularly difficult to implement.

In this letter, we report the direct observation of T vi-

olation in the B meson system, through the exchange of initial and final states in transitions that can only be connected by a T-symmetry transformation. The method is described in Ref. [15], based on the concepts proposed in Ref. [16] and further discussed in Refs. [11, 17, 18]. We use a data sample of 426 fb^{-1} of integrated luminosity at the $\Upsilon(4S)$ resonance, corresponding to 468×10^6 $B\overline{B}$ pairs, and 45 fb^{-1} at a center-of-mass (c.m.) energy 40 MeV below the $\Upsilon(4S)$, recorded by the *BABAR* detector [19] at the PEP-II asymmetric-energy e^+e^- collider at SLAC. The experimental analysis exploits identical reconstruction algorithms, selection criteria, calibration techniques, and B meson samples to our most recent time-dependent *CP* asymmetry measurement in $B \to c\overline{c}K^{(*)0}$ decays [20], with the exception of $\eta_c K^0_S$ and $J/\psi K^{*0}(\to K^0_S\pi^0)$ final states. The "flavor tagging" is combined here, for the first time, with the "*CP* tagging" [16], as required for the construction of T-transformed processes. Whereas the descriptions of the sample composition and time-dependent backgrounds are the same as described in Ref. [20], the signal giving access to the T-violating parameters needs a different data treatment. This echoes the fundamental differences between observables for T and *CP* symmetry breaking. The procedure to determine the T-violating parameters and their significance is thus novel [15].

In the decay of the $\Upsilon(4S)$, the two B mesons are in an entangled, antisymmetric state, as required by angular momentum conservation for a P-wave particle system. This two-body state is usually written in terms of flavor eigenstates, such as B^0 and $\overline{B}^0$, but can be expressed in terms of any linear combinations of B^0 and $\overline{B}^0$, such as the B_+ and B_- states introduced in Ref. [15]. They are defined as the neutral B states filtered by the decay to *CP*-eigenstates $J/\psi K^0_L$ (*CP*-even) and $J/\psi K^0_S$, with $K^0_S \to \pi\pi$ (*CP*-odd), respectively. The B_+ and B_- states are orthogonal to each other when there is only one weak phase involved in the B decay amplitude, as it occurs in B decays to $J/\psi K^0$ final states [21], and *CP* violation in neutral kaons is neglected.

We select events in which one B candidate is reconstructed in a B_+ or B_- state, and the flavor of the other B is identified, referred to as flavor identification (ID). We generically denote reconstructed final states that identify the flavor of the B as ℓ^-X for $\overline{B}^0$ and ℓ^+X for B^0. The notation (f_1, f_2) is used to indicate the flavor or *CP* final states that are reconstructed at corresponding times t_1 and t_2, where $t_2 > t_1$, i.e., $B_1 \to f_1$ is the first decay in the event and $B_2 \to f_2$ is the second decay. For later use in Eq. (1), we define $\Delta\tau = t_2 - t_1 > 0$. Once the B_1 state is filtered at time t_1, the living partner B_2 is prepared ("tagged") by entanglement as its orthogonal state. The notation $B_2(t_1) \to B_2(t_2)$ describes the transition of the B which decays at t_2, having tagged its state at t_1. For example, an event reconstructed in the time-ordered final states $(\ell^+X, J/\psi K^0_S)$ identifies the transition $\overline{B}^0 \to B_-$ for the second B to decay. We compare the rate for this transition to its T-reversed $B_- \to \overline{B}^0$ (exchange of initial and final states) by reconstructing the final states $(J/\psi K^0_L, \ell^-X)$. Any difference in these two rates is evidence for T-symmetry violation. There are three other independent comparisons that can be made between $B_+ \to B^0$ $(J/\psi K^0_S, \ell^+X)$, $\overline{B}^0 \to B_+$ $(\ell^+X, J/\psi K^0_L)$, and $B_- \to B^0$ $(J/\psi K^0_L, \ell^+X)$ transitions and their T-conjugates, $B^0 \to B_+$ $(\ell^-X, J/\psi K^0_L)$, $B_+ \to \overline{B}^0$ $(J/\psi K^0_S, \ell^-X)$, and $B^0 \to B_-$ $(\ell^-X, J/\psi K^0_S)$, respectively. Similarly, four different *CP* (*CPT*) comparisons can be made, e.g., between the $\overline{B}^0 \to B_-$ transition and its *CP* (*CPT*)-transformed $B^0 \to B_-$ $(B_- \to B^0)$ [15].

Assuming $\Delta\Gamma_d = 0$, each of the eight transitions has a general, time-dependent decay rate $g^{\pm}_{\alpha,\beta}(\Delta\tau)$ given by

$$e^{-\Gamma_d\Delta\tau}\big\{1 + S^{\pm}_{\alpha,\beta}\sin(\Delta m_d\Delta\tau) + C^{\pm}_{\alpha,\beta}\cos(\Delta m_d\Delta\tau)\big\}, \quad (1)$$

where indices $\alpha = \ell^+, \ell^-$ and $\beta = K^0_S, K^0_L$ stand for ℓ^+X, ℓ^-X and $c\overline{c}K^0_S, J/\psi K^0_L$ final states, respectively, and the symbol + or − indicates whether the decay to the flavor final state α occurs before or after the decay to the *CP* final state β. Here, Γ_d is the average decay width, Δm_d is the mass difference between the neutral B mass eigenstates, and $C^{\pm}_{\alpha,\beta}$ and $S^{\pm}_{\alpha,\beta}$ are model independent coefficients. The sine term, expected to be large in the SM, results from the interference between direct decay of the neutral B to the $J/\psi K^0$ final state and decay after B^0-$\overline{B}^0$ oscillation, while the cosine term arises from the interference between decay amplitudes with different weak and strong phases, and is expected to be negligible [21]. T violation would manifest itself through differences between the $S^{\pm}_{\alpha,\beta}$ or $C^{\pm}_{\alpha,\beta}$ values for T-conjugated processes, for example between $S^{+}_{\ell^+,K^0_S}$ and $S^{-}_{\ell^-,K^0_L}$.

In addition to $J/\psi K^0_S$, B_- states are reconstructed through the $\psi(2S)K^0_S$ and $\chi_{c1}K^0_S$ final states (denoted generically as $c\overline{c}K^0_S$), with $J/\psi, \psi(2S) \to e^+e^-, \mu^+\mu^-$, $\psi(2S) \to J/\psi\pi^+\pi^-$, $\chi_{c1} \to J/\psi\gamma$, and $K^0_S \to \pi^+\pi^-, \pi^0\pi^0$ (the latter only for $J/\psi K^0_S$). B_+ states are identified through $J/\psi K^0_L$. The $J/\psi K^0_L$ candidates are characterized by the difference ΔE between the reconstructed energy of the B and the beam energy in the e^+e^- c.m. frame, $E^*_{\rm beam}$, while for the $c\overline{c}K^0_S$ modes we use the beam-energy substituted invariant mass $m_{\rm ES} = \sqrt{(E^*_{\rm beam})^2 - (p^*_B)^2}$, where p^*_B is the B momentum in the c.m. frame.

The flavor ID of the other neutral B meson in the event, not associated with the reconstructed B_+ or B_-, is made on the basis of the charges of prompt leptons, kaons, pions from D^* mesons, and high-momentum charged particles. These flavor ID inputs are combined using a neural network (NN), trained with Monte Carlo (MC) simulated data. The output of the NN is then divided into six hierarchical, mutually exclusive flavor categories of increasing misidentification (misID) probability w. Events for which the NN output indicates very

low discriminating power are excluded from further analysis. We determine the signed difference of proper time $\Delta t = t_\beta - t_\alpha$ between the two B decays from the measured separation of the decay vertices along the collision axis. Events are accepted if the reconstructed $|\Delta t|$ and its estimated uncertainty, $\sigma_{\Delta t}$, are lower than 20 ps and 2.5 ps, respectively. The performances of the flavor ID and Δt reconstruction algorithms are evaluated by using a large sample of flavor-specific neutral B decays to $D^{(*)-}[\pi^+, \rho(770)^+, a_1(1260)^+]$ and $J/\psi K^{*0}(\to K^+\pi^-)$ final states (referred to as $B_{\rm flav}$ sample). The Δt resolution function is the same as in Ref. [20] except that all Gaussian offsets and widths are modeled to be proportional to $\sigma_{\Delta t}$.

The composition of the final sample is determined through fits to the $m_{\rm ES}$ and ΔE distributions, using parametric forms and distributions extracted from MC simulation and dilepton mass sidebands in data to describe the signal and background components. Figure 1 shows the $m_{\rm ES}$ and ΔE data distributions for events that satisfy the flavor ID and vertexing requirements, overlaid with the fit projections. The final sample contains 7796 $c\overline{c}K^0_S$ events, with purities in the signal region ($5.27 < m_{\rm ES} < 5.29$ GeV/c^2) ranging between 87% and 96%, and 5813 $J/\psi K^0_L$ events, with a purity of 56% in the $|\Delta E| < 10$ MeV region.

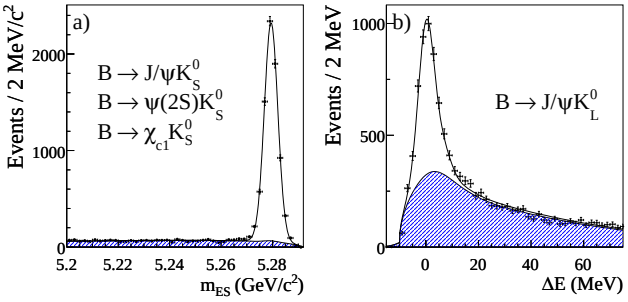

FIG. 1: (color online). Distributions of (a) $m_{\rm ES}$ and (b) ΔE for the neutral B decays reconstructed in the $c\overline{c}K^0_S$ and $J/\psi K^0_L$ final states, respectively, after flavor ID and vertexing requirements. In each plot, the shaded region is the estimated background contribution. The two samples of events are identical to those used in our most recent CP-violation study [20], but excluding $\eta_c K^0_S$ and $J/\psi K^{*0}(\to K^0_S\pi^0)$ final states.

We perform a simultaneous, unbinned maximum likelihood fit to the Δt distributions for flavor identified $c\overline{c}K^0_S$ and $J/\psi K^0_L$ events, split by flavor category. The signal probability density function (PDF) is [15]

$$\mathcal{H}_{\alpha,\beta}(\Delta t) \propto g^+_{\alpha,\beta}(\Delta t_{\rm true})H(\Delta t_{\rm true}) \otimes \mathcal{R}(\delta t;\sigma_{\Delta t}) + g^-_{\alpha,\beta}(-\Delta t_{\rm true})H(-\Delta t_{\rm true}) \otimes \mathcal{R}(\delta t;\sigma_{\Delta t}), \quad (2)$$

where $\Delta t_{\rm true}$ is the signed difference of proper time between the two B decays in the limit of perfect Δt reconstruction, H is the Heaviside step function, $\mathcal{R}(\delta t;\sigma_{\Delta t})$ with $\delta t = \Delta t - \Delta t_{\rm true}$ is the resolution function, and $g^\pm_{\alpha,\beta}$ are given by Eq. (1). Note that $\Delta t_{\rm true}$ is equivalent to $\Delta\tau$ ($-\Delta\tau$) when a true flavor (CP) tag occurs. Because of the convolution with the resolution function, the distribution for $\Delta t > 0$ contains predominantly true flavor-tagged events, with a small contribution from true CP-tagged events at low Δt, and conversely for $\Delta t < 0$. Mistakes in the flavor ID algorithm mix correct and incorrect flavor assignments, and dilute the T-violating asymmetries by a factor of approximately $(1-2w)$. Backgrounds are accounted for by adding terms to Eq. (2) [20]. Events are assigned signal and background probabilities based on the $m_{\rm ES}$ or ΔE distributions, for $c\overline{c}K^0_S$ or $J/\psi K^0_L$ events, respectively.

A total of 27 parameters are varied in the likelihood fit: eight pairs of $(S^\pm_{\alpha,\beta}, C^\pm_{\alpha,\beta})$ coefficients for the signal, and 11 parameters describing possible CP and T violation in the background. All remaining signal and background parameters are fixed to values taken from the $B_{\rm flav}$ sample, J/ψ-candidate sidebands in $J/\psi K^0_L$, world averages for Γ_d and Δm_d [22], or MC simulation [20]. From the 16 signal coefficients [23], we construct six pairs of independent asymmetry parameters $(\Delta S^\pm_T, \Delta C^\pm_T)$, $(\Delta S^\pm_{CP}, \Delta C^\pm_{CP})$, and $(\Delta S^\pm_{CPT}, \Delta C^\pm_{CPT})$, as shown in Table I. The T-asymmetry parameters have the advantage that T-symmetry breaking would directly manifest itself through any nonzero value of $\Delta S^\pm_T$ or $\Delta C^\pm_T$, or any difference between $\Delta S^\pm_{CP}$ and $\Delta S^\pm_{CPT}$, or between $\Delta C^\pm_{CP}$ and $\Delta C^\pm_{CPT}$ (analogously for CP- or CPT-symmetry breaking). The measured values for the asymmetry parameters are reported in Table I. There is another two times three pairs of T-, CP-, and CPT-asymmetry parameters, but they are not independent and can be derived from Table I or Ref. [23].

We build time-dependent asymmetries $A_T(\Delta t)$ to visually demonstrate the T-violating effect. For transition $\overline{B}^0 \to B_-$,

$$A_T(\Delta t) \equiv \frac{\mathcal{H}^-_{\ell^-,K^0_L}(\Delta t) - \mathcal{H}^+_{\ell^+,K^0_S}(\Delta t)}{\mathcal{H}^-_{\ell^-,K^0_L}(\Delta t) + \mathcal{H}^+_{\ell^+,K^0_S}(\Delta t)}\ , \quad (3)$$

where $\mathcal{H}^\pm_{\alpha,\beta}(\Delta t) = \mathcal{H}_{\alpha,\beta}(\pm\Delta t)H(\Delta t)$. With this construction, $A_T(\Delta t)$ is defined only for positive Δt values. Neglecting reconstruction effects, $A_T(\Delta t) \approx \frac{\Delta S^+_T}{2}\sin(\Delta m_d\Delta t) + \frac{\Delta C^+_T}{2}\cos(\Delta m_d\Delta t)$. We introduce the other three T-violating asymmetries similarly. Figure 2 shows the four observed asymmetries, overlaid with the projection of the best fit results to the Δt distributions with and without the eight T-invariance restrictions: $\Delta S^\pm_T = \Delta C^\pm_T = 0$, $\Delta S^\pm_{CP} = \Delta S^\pm_{CPT}$, and $\Delta C^\pm_{CP} = \Delta C^\pm_{CPT}$ [23].

Using large samples of MC simulated data, we determine that the asymmetry parameters are unbiased and have Gaussian errors. Splitting the data by flavor category or data-taking period give consistent results. Fitting a single pair of (S, C) coefficients, reversing the sign of S

TABLE I: Measured values of the T-, CP-, and CPT-asymmetry parameters, defined as the differences in $S^{\pm}_{\alpha,\beta}$ and $C^{\pm}_{\alpha,\beta}$ between symmetry-transformed transitions. The values of reference coefficients are also given at the bottom. The first uncertainty is statistical and the second systematic. The indices ℓ^-, ℓ^+, K^0_S, and K^0_L stand for reconstructed final states that identify the B meson as $\overline{B}^0$, B^0, B_-, and B_+, respectively.

Parameter	Result
$\Delta S^+_T = S^-_{\ell^-,K^0_L} - S^+_{\ell^+,K^0_S}$	$-1.37 \pm 0.14 \pm 0.06$
$\Delta S^-_T = S^+_{\ell^-,K^0_L} - S^-_{\ell^+,K^0_S}$	$1.17 \pm 0.18 \pm 0.11$
$\Delta C^+_T = C^-_{\ell^-,K^0_L} - C^+_{\ell^+,K^0_S}$	$0.10 \pm 0.14 \pm 0.08$
$\Delta C^-_T = C^+_{\ell^-,K^0_L} - C^-_{\ell^+,K^0_S}$	$0.04 \pm 0.14 \pm 0.08$
$\Delta S^+_{CP} = S^+_{\ell^-,K^0_S} - S^+_{\ell^+,K^0_S}$	$-1.30 \pm 0.11 \pm 0.07$
$\Delta S^-_{CP} = S^-_{\ell^-,K^0_S} - S^-_{\ell^+,K^0_S}$	$1.33 \pm 0.12 \pm 0.06$
$\Delta C^+_{CP} = C^+_{\ell^-,K^0_S} - C^+_{\ell^+,K^0_S}$	$0.07 \pm 0.09 \pm 0.03$
$\Delta C^-_{CP} = C^-_{\ell^-,K^0_S} - C^-_{\ell^+,K^0_S}$	$0.08 \pm 0.10 \pm 0.04$
$\Delta S^+_{CPT} = S^-_{\ell^+,K^0_L} - S^+_{\ell^+,K^0_S}$	$0.16 \pm 0.21 \pm 0.09$
$\Delta S^-_{CPT} = S^+_{\ell^+,K^0_L} - S^-_{\ell^+,K^0_S}$	$-0.03 \pm 0.13 \pm 0.06$
$\Delta C^+_{CPT} = C^-_{\ell^+,K^0_L} - C^+_{\ell^+,K^0_S}$	$0.14 \pm 0.15 \pm 0.07$
$\Delta C^-_{CPT} = C^+_{\ell^+,K^0_L} - C^-_{\ell^+,K^0_S}$	$0.03 \pm 0.12 \pm 0.08$
$S^+_{\ell^+,K^0_S}$	$0.55 \pm 0.09 \pm 0.06$
$S^-_{\ell^+,K^0_S}$	$-0.66 \pm 0.06 \pm 0.04$
$C^+_{\ell^+,K^0_S}$	$0.01 \pm 0.07 \pm 0.05$
$C^-_{\ell^+,K^0_S}$	$-0.05 \pm 0.06 \pm 0.03$

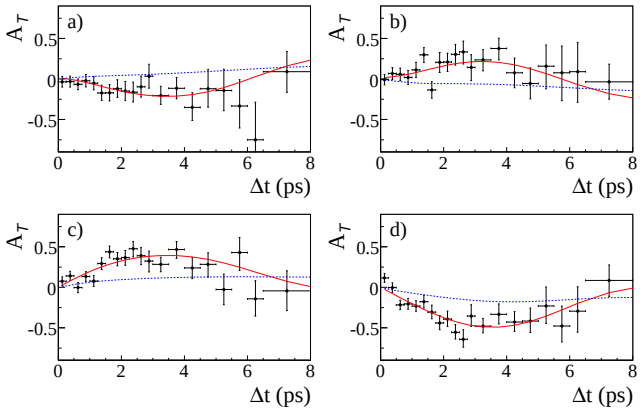

FIG. 2: (color online). The four independent T-violating asymmetries for transition a) $\overline{B}^0 \to B_-$ $(\ell^+X, c\overline{c}K^0_S)$, b) $B_+ \to B^0$ $(c\overline{c}K^0_S, \ell^+X)$, c) $\overline{B}^0 \to B_+$ $(\ell^+X, J/\psi K^0_L)$, d) $B_- \to B^0$ $(J/\psi K^0_L, \ell^+X)$, for combined flavor categories with low misID (leptons and kaons), in the signal region ($5.27 < m_{\rm ES} < 5.29$ GeV/c^2 for $c\overline{c}K^0_S$ modes and $|\Delta E| < 10$ MeV for $J/\psi K^0_L$). The points with error bars represent the data, the red solid and dashed blue curves represent the projections of the best fit results with and without T violation, respectively.

under $\Delta t \leftrightarrow -\Delta t$, or $B_+ \leftrightarrow B_-$ or $B^0 \leftrightarrow \overline{B}^0$ exchanges, and the sign of C under $B^0 \leftrightarrow \overline{B}^0$ exchange, we obtain identical results to those obtained in Ref. [20]. Performing the analysis with B decays to $c\overline{c}K^{\pm}$ and $J/\psi K^{*\pm}$ final states instead of the signal $c\overline{c}K^0_S$ and $J/\psi K^0_L$, respectively, we find that all the asymmetry parameters are consistent with zero.

In evaluating systematic uncertainties in the asymmetry parameters, we follow the same procedure as in Ref. [20], with small changes [23]. We considered the statistical uncertainties on the flavor misID probabilities, Δt resolution function, and $m_{\rm ES}$ parameters. Differences in the misID probabilities and Δt resolution function between $B_{\rm flav}$ and CP final states, uncertainties due to assumptions in the resolution for signal and background components, compositions of the signal and backgrounds, the $m_{\rm ES}$ and ΔE PDFs, and the branching fractions for the backgrounds and their CP properties, have also been accounted for. We also assign a systematic uncertainty corresponding to any deviation of the fit for MC simulated asymmetry parameters from their generated MC values, taking the largest between the deviation and its statistical uncertainty. Other sources of uncertainty such as our limited knowledge of Γ_d, Δm_d, and other fixed parameters, the interaction region, the detector alignment, and effects due to a nonzero $\Delta\Gamma_d$ value in the time dependence and the normalization of the PDF, are also considered. Treating $c\overline{c}K^0_S$ and $J/\psi K^0_L$ as orthogonal states and neglecting CP violation for flavor categories without leptons, has an impact well below the statistical uncertainty. The total systematic uncertainties are shown in Table I [23].

The significance of the T-violation signal is evaluated based on the change in log-likelihood with respect to the maximum ($-2\Delta\ln\mathcal{L}$). We reduce $-2\Delta\ln\mathcal{L}$ by a factor $1 + \max\{m_i^2\} = 1.61$ to account for systematic errors in the evaluation of the significance. Here, $m_i^2 = -2(\ln\mathcal{L}_i - \ln\mathcal{L})/s^2$, where $\ln\mathcal{L}$ is the maximum log-likelihood, $\ln\mathcal{L}_i$ is the log-likelihood with asymmetry parameter i fixed to its total systematic variation and maximized over all other parameters, and $s^2 \approx 1$ is the change in $2\ln\mathcal{L}$ at 68% confidence level (CL) for one degree of freedom (d.o.f). Figure 3 shows CL contours calculated from the change $-2\Delta\ln\mathcal{L}$ in two dimensions for the T-asymmetry parameters $(\Delta S^+_T, \Delta C^+_T)$ and $(\Delta S^-_T, \Delta C^-_T)$. The difference in the value of $2\ln\mathcal{L}$ at the best fit solution with and without T violation is 226 with eight d.o.f., including systematic uncertainties. Assuming Gaussian errors, this corresponds to a significance equivalent to 14.0 standard deviations (σ), and thus constitutes direct observation of T violation. The significance of CP and CPT violation is determined analogously, obtaining 307

and 5, respectively, equivalent to 17σ and 0.3σ, consistent with *CP* violation and *CPT* invariance.

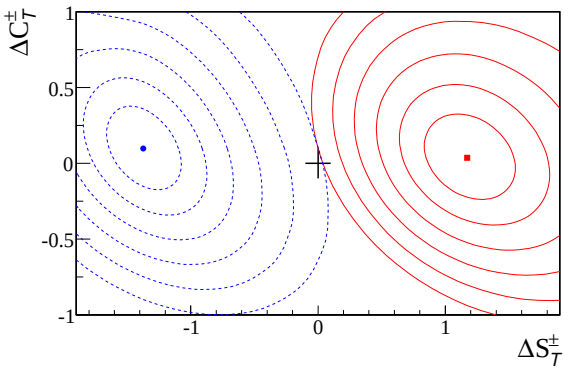

FIG. 3: (color online). The central values (blue point and red square) and two-dimensional CL contours for $1-\mathrm{CL} = 0.317,\ 4.55\times10^{-2},\ 2.70\times10^{-3},\ 6.33\times10^{-5},\ 5.73\times10^{-7}$, and 1.97×10^{-9}, calculated from the change in the value of $-2\Delta\ln\mathcal{L}$ compared with its value at maximum ($-2\Delta\ln\mathcal{L} = 2.3, 6.2, 11.8, 19.3, 28.7, 40.1$), for the pairs of T-asymmetry parameters $(\Delta S_T^+, \Delta C_T^+)$ (blue dashed curves) and $(\Delta S_T^-, \Delta C_T^-)$ (red solid curves). Systematic uncertainties are included. The T-invariance point is shown as a + sign.

In summary, we have measured T-violating parameters in the time evolution of neutral B mesons, by comparing the probabilities of $\overline{B}^0 \to B_-$, $B_+ \to B^0$, $\overline{B}^0 \to B_+$, and $B_- \to B^0$ transitions, to their T conjugate. We determine for the main T-violating parameters $\Delta S_T^+ = -1.37 \pm 0.14$ (stat.) $\pm$ 0.06 (syst.) and $\Delta S_T^- = 1.17 \pm 0.18$ (stat.) $\pm$ 0.11 (syst.), and observe directly for the first time a departure from T invariance in the B meson system, with a significance equivalent to 14σ. Our results are consistent with current *CP*-violating measurements obtained invoking *CPT* invariance. They constitute the first observation of T violation in any system through the exchange of initial and final states in transitions that can only be connected by a T-symmetry transformation.

We are grateful for the excellent luminosity and machine conditions provided by our PEP-II colleagues, and for the substantial dedicated effort from the computing organizations that support *BABAR*. The collaborating institutions wish to thank SLAC for its support and kind hospitality. This work is supported by DOE and NSF (USA), NSERC (Canada), CEA and CNRS-IN2P3 (France), BMBF and DFG (Germany), INFN (Italy), FOM (The Netherlands), NFR (Norway), MES (Russia), MICIIN (Spain), STFC (United Kingdom). Individuals have received support from the Marie Curie EIF (European Union), the A. P. Sloan Foundation (USA) and the Binational Science Foundation (USA-Israel).

* Now at the University of Tabuk, Tabuk 71491, Saudi Arabia
† Also with Università di Perugia, Dipartimento di Fisica, Perugia, Italy
‡ Now at the University of Huddersfield, Huddersfield HD1 3DH, UK
§ Deceased
¶ Now at University of South Alabama, Mobile, Alabama 36688, USA
** Also with Università di Sassari, Sassari, Italy

[1] J.H. Christenson *et al.*, Phys. Rev. Lett. **13**, 138 (1964).
[2] B. Aubert *et al.* (*BABAR* Collaboration), Phys. Rev. Lett. **87**, 091801 (2001); K. Abe *et al.* (Belle Collaboration), Phys. Rev. Lett. **87**, 091802 (2001).
[3] B. Aubert *et al.* (*BABAR* Collaboration), Phys. Rev. Lett. **93**, 131801 (2004); Y. Chao *et al.* (Belle Collaboration), Phys. Rev. Lett. **93**, 191802 (2004).
[4] N. Cabibbo, Phys. Rev. Lett. **10**, 531 (1963); M. Kobayashi and T. Maskawa, Prog. Theor. Phys. **49**, 652 (1973).
[5] G. Lüders, Math. Fysik. Medd. Kgl. Danske Akad. Ved. Volume 28, 1954, p. 5; J.S. Bell, Birmingham University thesis (1954); W. Pauli, in W. Pauli, ed., Niels Bohr and the Development of Physics (McGraw-Hill, NY, 1955).
[6] R. Carosi *et al.*, Phys. Lett. B **237**, 303 (1990); A. Alavi-Harati *et al.*, Phys. Rev. D **67**, 012005 (2003); B. Schwingenheuer *et al.*, Phys. Rev. Lett. **74**, 4376 (1995).
[7] See "Tests of conservation laws" review in [22].
[8] A. Angelopoulus *et al.* (CPLEAR Collaboration), Phys. Lett. B **444**, 43 (1998).
[9] P. K. Kabir, Phys. Rev. D **2**, 540 (1970).
[10] L. Wolfenstein, Phys. Rev. Lett. **83**, 911 (1999).
[11] L. Wolfenstein, Int. Jour. Mod. Phys. **8**, 501 (1999).
[12] H.J. Gerber, Eur. Phys. Jour. C **35**, 195 (2004), and references therein.
[13] B. Aubert *et al.* (*BABAR* Collaboration), Phys. Rev. Lett. **96**, 251802 (2006), Phys. Rev. Lett. **92**, 181801 (2004); E. Nakano *et al.* (Belle Collaboration), Phys. Rev. D **73**, 112002 (2006); V.M. Abazov *et al.* (D0 Collaboration), Phys. Rev. Lett. **105**, 081801 (2010), Phys. Rev. Lett. **98**, 151801 (2007); F. Abe *et al.* (CDF Collaboration), Phys. Rev. D **55**, 2546 (2006).
[14] J.J. Hudson *et al.*, Nature **473**, 493-496 (2011); C.A. Baker *et al.*, Phys. Rev. Lett. **97**, 131801 (2006).
[15] J. Bernabeu, F. Martinez-Vidal, P. Villanueva-Perez, JHEP **1208**, 064 (2012).
[16] M. C. Bañuls and J. Bernabeu, Phys. Lett. B **464**, 117 (1999); Nucl. Phys. B **590**, 19 (2000).
[17] H. R. Quinn, J. Phys. Conf. Ser. **171**, 011001 (2009).
[18] J. Bernabeu, J. Phys. Conf. Ser. **335**, 012011 (2011).
[19] B. Aubert *et al.* (*BABAR* Collaboration), Nucl. Instrum. Methods Phys. Res., Sect. A **479**, 1 (2002).
[20] B. Aubert *et al.* (*BABAR* Collaboration), Phys. Rev. D **79**, 072009 (2009).
[21] See "*CP* violation in meson decays" review in [22].
[22] K. Nakamura *et al.* (Particle Data Group), J. Phys. **G37**, 075021 (2010).
[23] See supplementary material for breakdown of the main systematic uncertainties on the asymmetry parameters, *CP*- and *CPT*-violating asymmetries, and complete $(S_{\alpha,\beta}^{\pm}, C_{\alpha,\beta}^{\pm})$ analysis results.

Observation of Time Reversal Violation in the B^0 Meson System

The *BABAR* Collaboration

The following includes supplementary material for the Electronic Physics Auxiliary Publication Service.

TABLE I: Breakdown of main systematic uncertainties on the T-, CP-, and CPT-asymmetry parameters and the $(S^{\pm}_{\ell^+,K^0_S}, C^{\pm}_{\ell^+,K^0_S})$ coefficients for $\overline{B}^0 \to B_-$ and $B_+ \to B^0$ transitions. The indices ℓ^+ and K^0_S stand for reconstructed final states that identify the B meson as B^0 and B_-, respectively. The first nine rows in each panel are evaluated using similar procedures as in Ref. [20]. The tenth and eleventh rows ($\Delta\Gamma_d/\Gamma_d$ and PDF normalization) are estimated by varying $\Delta\Gamma_d/\Gamma_d$ by $\pm 2\%$, while the $\sinh(\Delta\Gamma\Delta\tau)$ and $\cosh(\Delta\Gamma\Delta\tau)$ coefficients of the most general time-dependent decay rate $g^{\pm}_{\alpha,\beta}(\Delta\tau)$ [15] are changed around their reference model values, 0 and 1, respectively. The PDF normalization also accounts for systematic effects related to the Δt range used to normalize the PDF. The total systematic uncertainty (last row in each panel) is calculated adding the individual systematic uncertainties in quadrature.

Systematic source	ΔS^+_T	ΔS^-_T	ΔC^+_T	ΔC^-_T	ΔS^+_{CP}	ΔS^-_{CP}	ΔC^+_{CP}	ΔC^-_{CP}
Interaction region	0.011	0.035	0.02	0.029	0.012	0.024	0.015	0.026
Flavor misID probabilities	0.022	0.042	0.022	0.022	0.016	0.040	0.020	0.020
Δt resolution	0.030	0.050	0.048	0.062	0.057	0.033	0.012	0.011
$J/\psi\, K^0_L$ background	0.033	0.038	0.052	0.010	0.002	0.001	0.001	0.002
Background fractions and CP content	0.029	0.021	0.020	0.026	0.013	0.012	0.008	0.009
$m_{\rm ES}$ parameterization	0.011	0.002	0.005	0.002	0.016	0.008	0.005	0.004
Γ_d and Δm_d	0.001	0.005	0.011	0.008	0.003	0.007	0.011	0.012
CP violation for flavor ID categories	0.018	0.019	0.001	0.001	0.009	0.008	0.006	0.006
Fit bias	0.010	0.072	0.013	0.010	0.010	0.007	0.007	0.014
$\Delta\Gamma_d/\Gamma_d$	0.004	0.003	0.002	0.002	0.004	0.003	0.001	0.001
PDF normalization	0.013	0.019	0.005	0.004	0.017	0.012	0.006	0.007
Total	0.064	0.112	0.08	0.077	0.068	0.061	0.033	0.041

Systematic source	ΔS^+_{CPT}	ΔS^-_{CPT}	ΔC^+_{CPT}	ΔC^-_{CPT}	$S^+_{\ell^+,K^0_S}$	$S^-_{\ell^+,K^0_S}$	$C^+_{\ell^+,K^0_S}$	$C^-_{\ell^+,K^0_S}$
Interaction region	0.015	0.024	0.023	0.026	0.014	0.009	0.015	0.008
Flavor misID probabilities	0.018	0.008	0.009	0.009	0.013	0.020	0.012	0.010
Δt resolution	0.062	0.033	0.051	0.072	0.051	0.030	0.045	0.012
$J/\psi\, K^0_L$ background	0.046	0.021	0.029	0.015	0.002	0.001	0.001	0.001
Background fractions and CP content	0.024	0.020	0.024	0.016	0.012	0.004	0.007	0.007
$m_{\rm ES}$ parameterization	0.011	0.002	0.005	0.002	0.011	0.002	0.005	0.002
Γ_d and Δm_d	0.004	0.001	0.002	0.003	0.003	0.003	0.009	0.008
CP violation for flavor ID categories	0.026	0.010	0.007	0.005	0.014	0.005	0.003	0.002
Fit bias	0.018	0.026	0.007	0.021	0.005	0.017	0.006	0.015
$\Delta\Gamma_d/\Gamma_d$	0.003	0.002	0.002	0.001	0.002	0.001	0.001	0.001
PDF normalization	0.019	0.015	0.007	0.004	0.008	0.002	0.003	0.003
Total	0.092	0.058	0.067	0.083	0.059	0.041	0.051	0.026

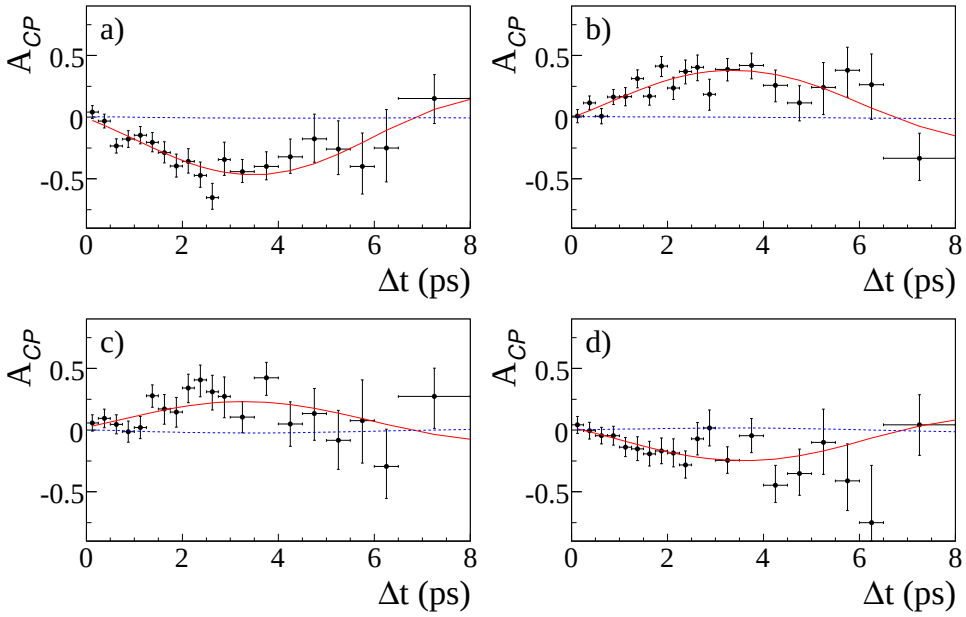

FIG. 1: (color online). The four independent *CP*-violating asymmetries for transition a) $\overline{B}^0 \to B_-$ $(\ell^+X, c\overline{c}K^0_S)$, b) $B_+ \to B^0$ $(c\overline{c}K^0_S, \ell^+X)$, c) $\overline{B}^0 \to B_+$ $(\ell^+X, J/\psi\, K^0_L)$, d) $B_- \to B^0$ $(J/\psi\, K^0_L, \ell^+X)$, for combined flavor categories with low misID (leptons and kaons), in the signal region ($5.27 < m_{\rm ES} < 5.29$ GeV/c^2 for $c\overline{c}K^0_S$ modes and $|\Delta E| < 10$ MeV for $J/\psi\, K^0_L$). The points with error bars represent the data, the red solid and dashed blue curves represent the projections of the best fit results with and without *CP* violation, respectively.

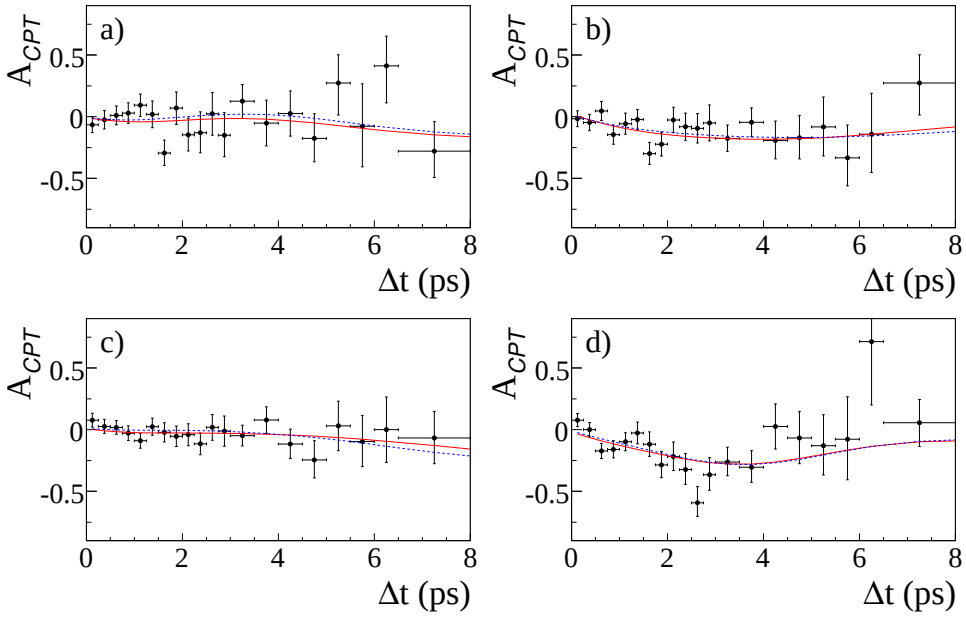

FIG. 2: (color online). The four independent *CPT*-violating asymmetries for transition a) $B_+ \to B^0$ $(c\overline{c}K^0_S, \ell^+X)$, b) $B_+ \to \overline{B}^0$ $(c\overline{c}K^0_S, \ell^-X)$, c) $B_- \to B^0$ $(J/\psi\, K^0_L, \ell^+X)$, d) $B_- \to \overline{B}^0$ $(J/\psi\, K^0_L, \ell^-X)$, for combined flavor categories with low misID (leptons and kaons), in the signal region ($5.27 < m_{\rm ES} < 5.29$ GeV/c^2 for $c\overline{c}K^0_S$ modes and $|\Delta E| < 10$ MeV for $J/\psi\, K^0_L$). The points with error bars represent the data, the red solid and dashed blue curves represent the projections of the best fit results with and without *CPT* violation, respectively.

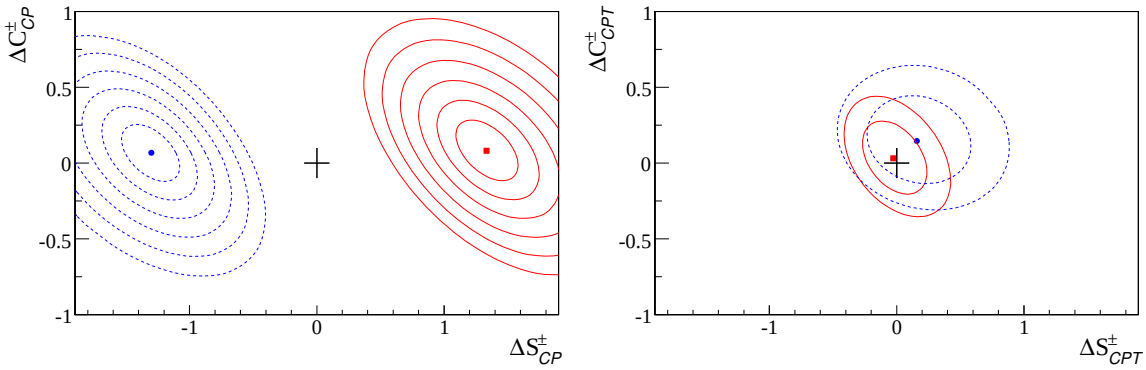

FIG. 3: (color online). The central values (blue point and red square) and two-dimensional CL contours for $1 - \mathrm{CL} = 0.317$, 4.55×10^{-2}, 2.70×10^{-3}, 6.33×10^{-5}, 5.73×10^{-7}, and 1.97×10^{-9}, calculated from the change in the value of $-2\Delta \ln \mathcal{L}$ compared with its value at maximum, for the pairs of CP- (left) and CPT- (right) asymmetry parameters $(\Delta S^{+}_{CP}, \Delta C^{+}_{CP})$ and $(\Delta S^{+}_{CPT}, \Delta C^{+}_{CPT})$ (blue dashed curves) and $(\Delta S^{-}_{CP}, \Delta C^{-}_{CP})$, $(\Delta S^{-}_{CPT}, \Delta C^{-}_{CPT})$ (red solid curves). Systematic uncertainties are included. The CP- and CPT-invariance points are shown as a plus sign (+).

TABLE II: Measured values of the $(S^{\pm}_{\alpha,\beta}, C^{\pm}_{\alpha,\beta})$ coefficients. The first uncertainty is statistical and the second systematic. The indices $\alpha = \ell^-, \ell^+$ and $\beta = K^0_S, K^0_L$ stand for reconstructed final states that identify the B meson as $\overline{B}^0$, B^0 and B_-, B_+, respectively.

Transition		Parameter	Result
$B_- \to \overline{B}^0$	$(J/\psi\, K^0_L, \ell^- X)$	$S^-_{\ell^-,K^0_L}$	$-0.83 \pm 0.11 \pm 0.06$
$B^0 \to B_-$	$(\ell^- X, c\bar{c} K^0_S)$	$S^+_{\ell^-,K^0_S}$	$-0.76 \pm 0.06 \pm 0.04$
$B_- \to B^0$	$(J/\psi\, K^0_L, \ell^+ X)$	$S^-_{\ell^+,K^0_L}$	$0.70 \pm 0.19 \pm 0.12$
$\overline{B}^0 \to B_-$	$(\ell^+ X, c\bar{c} K^0_S)$	$S^+_{\ell^+,K^0_S}$	$0.55 \pm 0.09 \pm 0.06$
$B^0 \to B_+$	$(\ell^- X, J/\psi\, K^0_L)$	$S^+_{\ell^-,K^0_L}$	$0.51 \pm 0.17 \pm 0.11$
$B_+ \to \overline{B}^0$	$(c\bar{c} K^0_S, \ell^- X)$	$S^-_{\ell^-,K^0_S}$	$0.67 \pm 0.10 \pm 0.08$
$\overline{B}^0 \to B_+$	$(\ell^+ X, J/\psi\, K^0_L)$	$S^+_{\ell^+,K^0_L}$	$-0.69 \pm 0.11 \pm 0.04$
$B_+ \to B^0$	$(c\bar{c} K^0_S, \ell^+ X)$	$S^-_{\ell^+,K^0_S}$	$-0.66 \pm 0.06 \pm 0.04$
$B_- \to \overline{B}^0$	$(J/\psi\, K^0_L, \ell^- X)$	$C^-_{\ell^-,K^0_L}$	$0.11 \pm 0.12 \pm 0.08$
$B^0 \to B_-$	$(\ell^- X, c\bar{c} K^0_S)$	$C^+_{\ell^-,K^0_S}$	$0.08 \pm 0.06 \pm 0.06$
$B_- \to B^0$	$(J/\psi\, K^0_L, \ell^+ X)$	$C^-_{\ell^+,K^0_L}$	$0.16 \pm 0.13 \pm 0.06$
$\overline{B}^0 \to B_-$	$(\ell^+ X, c\bar{c} K^0_S)$	$C^+_{\ell^+,K^0_S}$	$0.01 \pm 0.07 \pm 0.05$
$B^0 \to B_+$	$(\ell^- X, J/\psi\, K^0_L)$	$C^+_{\ell^-,K^0_L}$	$-0.01 \pm 0.13 \pm 0.08$
$B_+ \to \overline{B}^0$	$(c\bar{c} K^0_S, \ell^- X)$	$C^-_{\ell^-,K^0_S}$	$0.03 \pm 0.07 \pm 0.04$
$\overline{B}^0 \to B_+$	$(\ell^+ X, J/\psi\, K^0_L)$	$C^+_{\ell^+,K^0_L}$	$-0.02 \pm 0.11 \pm 0.08$
$B_+ \to B^0$	$(c\bar{c} K^0_S, \ell^+ X)$	$C^-_{\ell^+,K^0_S}$	$-0.05 \pm 0.06 \pm 0.03$

TABLE III: Statistical correlation coefficients for the vector of $(S^{\pm}_{\alpha,\beta}, C^{\pm}_{\alpha,\beta})$ measurements given in the same order as in Table II. Only lower off-diagonal terms are written, in %.

$$\begin{pmatrix}
100 & & & & & & & & & & & & & & & \\
0 & 100 & & & & & & & & & & & & & & \\
-14 & 0 & 100 & & & & & & & & & & & & & \\
2 & -6 & 0 & 100 & & & & & & & & & & & & \\
8 & 0 & 41 & 0 & 100 & & & & & & & & & & & \\
0 & 18 & 0 & 38 & 0 & 100 & & & & & & & & & & \\
6 & 0 & 19 & 0 & -7 & 0 & 100 & & & & & & & & & \\
0 & 10 & 0 & 16 & 0 & -9 & 1 & 100 & & & & & & & & \\
-45 & 0 & 38 & -1 & 31 & 0 & 9 & 0 & 100 & & & & & & & \\
0 & -33 & 0 & 31 & 0 & 28 & 0 & 6 & 0 & 100 & & & & & & \\
27 & 0 & -9 & 0 & 23 & 0 & 18 & 0 & -14 & 0 & 100 & & & & & \\
0 & 28 & 0 & -14 & 0 & 23 & 0 & 18 & 1 & -15 & 0 & 100 & & & & \\
15 & 0 & 21 & 0 & -21 & 0 & 27 & 0 & -16 & 0 & 22 & 0 & 100 & & & \\
0 & 18 & 0 & 21 & 0 & -18 & 0 & 29 & 0 & -16 & 0 & 21 & 0 & 100 & & \\
1 & 0 & 25 & 0 & 31 & 0 & -37 & 0 & 22 & 0 & -15 & 0 & -20 & 0 & 100 & \\
0 & 7 & 0 & 23 & 0 & 31 & 0 & -41 & 0 & 20 & 0 & -17 & 0 & -20 & 0 & 100
\end{pmatrix}$$

TABLE IV: Systematic correlation coefficients for the vector of $(S^{\pm}_{\alpha,\beta}, C^{\pm}_{\alpha,\beta})$ measurements given in the same order as in Table II. Only lower off-diagonal terms are written, in %.

$$\begin{pmatrix}
100 & & & & & & & & & & & & & & & \\
6 & 100 & & & & & & & & & & & & & & \\
18 & -14 & 100 & & & & & & & & & & & & & \\
44 & 3 & 66 & 100 & & & & & & & & & & & & \\
16 & -4 & 57 & 58 & 100 & & & & & & & & & & & \\
37 & -19 & 67 & 66 & 44 & 100 & & & & & & & & & & \\
-5 & -5 & 10 & 8 & -4 & -3 & 100 & & & & & & & & & \\
30 & -19 & 57 & 59 & 10 & 58 & 6 & 100 & & & & & & & & \\
-28 & -10 & 39 & 13 & 43 & 21 & -8 & -1 & 100 & & & & & & & \\
42 & -20 & 60 & 68 & 57 & 72 & -6 & 47 & 30 & 100 & & & & & & \\
-31 & 0 & 23 & 17 & 20 & 8 & 11 & 6 & 58 & 18 & 100 & & & & & \\
41 & -27 & 70 & 66 & 46 & 64 & 0 & 71 & 32 & 81 & 20 & 100 & & & & \\
31 & -16 & 63 & 63 & 39 & 67 & -23 & 59 & 39 & 63 & 24 & 73 & 100 & & & \\
1 & -1 & 15 & 7 & 2 & 2 & -31 & 5 & 23 & 7 & 5 & 18 & 49 & 100 & & \\
28 & -23 & 73 & 72 & 52 & 61 & -1 & 64 & 43 & 69 & 28 & 84 & 83 & 39 & 100 & \\
-14 & -13 & 12 & -6 & -34 & 11 & 2 & 34 & 23 & 0 & 31 & 17 & 26 & 15 & 15 & 100
\end{pmatrix}$$